Optical absorption and activated transport in polaronic systems

G. Schubert,[1] G. Wellein,[2] A. Weisse,[3] A. Alvermann,[1] and H. Fehske[1]

[1]*Institut für Physik, Ernst Moritz Arndt Universität Greifswald, 17487 Greifswald, Germany*
[2]*Regionales Rechenzentrum Erlangen, Universität Erlangen, 91058 Erlangen, Germany*
[3]*School of Physics, The University of New South Wales, Sydney, NSW 2052, Australia*

We present exact results for the optical response in the one-dimensional Holstein model. In particular, by means of a refined kernel polynomial method, we calculate the ac and dc electrical conductivities at finite temperatures for a wide parameter range of electron-phonon interaction. We analyze the deviations from the results of standard small polaron theory in the intermediate coupling regime and discuss nonadiabaticity effects in detail.

I. INTRODUCTION

The investigation of transport properties has been playing a central role in condensed matter physics for a long time. In recent years optical spectroscopy, for example, has contributed a lot to unravel the complex physics of highly correlated many-body systems, such as the one-dimensional (1D) metal-halogenide complexes,[1] the quasi-two-dimensional (2D) high-temperature superconducting cuprates,[2] or the three-dimensional (3D) colossal magnetoresistive manganites.[3] That way, optical measurements proved the importance of electron-phonon (EP) interactions in all these materials and, in particular, corroborated polaronic scenarios for modeling their electronic transport properties at least at high temperatures.[4–6]

Polarons are quasiparticles composed of an electron and the surrounding ions which, in a polar solid, provided the electron lattice interaction is sufficiently strong, are displaced from their equilibrium positions due to the presence of the electron. This bootstrap relation between electron and lattice displacement makes the particle heavy, because it has to drag with it the potential well of the phonons. Polaron motion is largely understood and has been worked out theoretically in two important limits. In the first case, the electronic bandwidth is large and there is a only a slight change in the particle's effective mass due to the EP coupling. These quasiparticles are called large polarons or Fröhlich polarons. In the second case it is assumed that the bandwidth is small, whereas the EP interaction is strong and short ranged. Now polaronic effects trap the electron at a certain lattice site and the size of the quasiparticle becomes comparable to the interatomic lattice spacing. Thermally activated hopping will necessarily be the dominant transport process of such small or Holstein-type polarons. Although there are experimental systems with clear large and small polaron characteristics, most of the above-mentioned novel materials belong to the transition region between these two limiting cases. Here, the relevant energy scales are not well separated and perturbative approaches cannot describe the complicated transport mechanisms adequately.

A recent nonperturbative dynamical mean-field (DMFT) study of the Holstein model in infinite dimensions[7] reports quantitative discrepancies of the temperature dependence of the resistivity from standard polaron formulas, but the dynamical mean-field approach inherently does not account for vertex corrections to the conductivity and for longer ranged hopping processes induced by the EP interaction. On the other hand, exact numerical investigations of the Holstein model provided quite a number of reliable results for the zero-temperature optical conductivity in the 1D and 2D (extended) Holstein models.[8,9]

Motivated by this situation, in the present work we use a recently developed extension of the kernel polynomial method (KPM),[10,11] a refined numerical Chebyshev expansion technique, to compute both the dc and ac hopping conductivities at finite temperatures without any serious approximation.

II. MODEL AND METHOD

Our starting point is the 1D tight-binding Holstein Hamiltonian,[12]

$$H = -t \sum_{\langle i,j \rangle} c_i^\dagger c_j - \sqrt{\varepsilon_p \omega_0} \sum_i (b_i^\dagger + b_i) n_i + \hbar \omega_0 \sum_i b_i^\dagger b_i, \quad (1)$$

describing a single electron coupled locally to a dispersionless optical phonon mode, where $c_i^\dagger$ ($b_i^\dagger$) denotes the corresponding fermionic (bosonic) creation operator, and $n_i = c_i^\dagger c_i$. Setting $\hbar = 1$ and measuring all energies in units of the nearest-neighbor hopping integral t, the physics of the model is determined by the dimensionless EP coupling constants

$$\lambda = \varepsilon_p/2t \quad \text{and} \quad g^2 = \varepsilon_p/\omega_0 \quad (2)$$

in the adiabatic ($\omega_0/t \ll 1$) and antiadiabatic ($\omega_0/t \gg 1$) regimes, respectively. In 1D the crossover from large to small polaron behavior takes place at $\lambda \simeq 1$ ($g^2 \simeq 1$) in the former (latter) case.[13,14] Whether large polarons form in the Holstein model for $D > 1$ is still under debate.[15–17]

Addressing the linear response of our system to an external (longitudinal) electric field we consider the Kubo formula for the electrical conductivity at finite temperatures, which is[18]

$$\text{Re }\sigma(\omega) = \pi \sum_{m,n}^{\infty} \frac{e^{-\beta E_n} - e^{-\beta E_m}}{ZL\omega} |\langle n|\hat{j}|m\rangle|^2 \delta(\omega - \omega_{mn}). \quad (3)$$

Here $Z = \sum_n^\infty e^{-\beta E_n}$ is the partition function and $\beta = T^{-1}$ denotes the inverse temperature. Since the Holstein Hamiltonian (1) involves bosonic degrees of freedom, the Hilbert space even of a finite L-site system has infinite dimension. In practice, however, the contribution of highly excited phonon states is negligible at the relevant temperatures, and the system is well approximated by a truncated phonon space with at most $M(\lambda, g, \omega_0; T)$ phonons.[19] Then $|n\rangle$ and $|m\rangle$ are the eigenstates of H within our truncated D-dimensional Hilbert space, E_n and E_m are the corresponding eigenvalues, and $\omega_{mn} = E_m - E_n$. In Eq. (3) the current operator has the standard hopping form, $\hat{j} = iet\sum_i(c_i^\dagger c_{i+1} - c_{i+1}^\dagger c_i)$, and connects states with different parity.[20] Thus, assuming that the ground state is nondegenerate, the expectation value $\langle 0|\hat{j}|0\rangle$ vanishes in the absence of an external electric field. The limit $\omega \to 0$ of (3) yields the dc conductivity, whereas the optical absorption is given by the finite frequency data. For small polarons both results are interesting and have been evaluated analytically at an early stage.[21] At $T=0$, the regular part of the optical conductivity, $\sigma^{\text{reg}}(\omega) = (\pi/L)\sum_{n>0}\omega_{n0}^{-1}|\langle n|\hat{j}|0\rangle|^2\delta(\omega - \omega_{n0})$, was calculated for finite 1D and 2D lattices with periodic boundary conditions (PBC) in a wide parameter range of the Holstein model, using a combination of the Lanczos algorithm and the KPM.[8]

At finite temperatures, a similar straightforward expansion of the conductivity is spoiled by the presence of the Boltzmann factors and the contribution of all matrix elements between eigenstates of the system. Instead, it turns out that a generalized KPM scheme[11,22] can be based upon a current operator density

$$j(x,y) = \sum_{m,n} |\langle n|\hat{j}|m\rangle|^2 \delta(x - E_n) \delta(y - E_m). \quad (4)$$

Being a function of two variables, $j(x,y)$ can be expanded by a two-dimensional KPM,

$$\tilde{j}(x,y) = \sum_{k,l=0}^{N-1} \frac{\mu_{kl} w_{kl} g_k^J g_l^J T_k(x) T_l(y)}{\pi^2 \sqrt{(1-x^2)(1-y^2)}}, \quad (5)$$

where the tilde refers to a rescaling of energy $(H \to \tilde{H})$ that maps the spectrum of H into the domain $[-1,1]$ of the Chebyshev polynomials of first kind $T_k(x)$. The finite order N of the expansion leads to Gibbs oscillations which can be damped by introducing appropriate damping factors. Here we use g_n^J derived from the Jackson kernel[10,23] and $N=512$ throughout the paper. The core of the numerical work is the iterative calculation of the moments $\mu_{kl} = \text{Tr}[T_k(\tilde{H})\hat{j}T_l(\tilde{H})\hat{j}]$, where the trace can be replaced by an average over a relatively small number of random vectors $|r\rangle$.[24] Finally, the factors $1/w_{kl} = (2-\delta_{k0})(2-\delta_{l0})$ account for the correct normalization. Given the operator density $j(x,y)$ we find the optical conductivity by integration
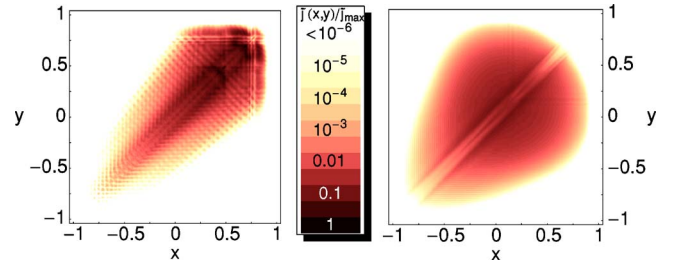

FIG. 1. (Color online) Renormalized current operator density $\tilde{j}(x,y)$ used in the 2D KPM. Data obtained for the 1D Holstein model with $\lambda = 0.2$ (left panel) and $\lambda = 2.0$ (right panel) at $\omega_0/t = 0.4$ ($L=6$, $M=50$; PBC).

$$\text{Re }\sigma(\omega) = \frac{\pi}{ZL\omega} \int_{-\infty}^{\infty} j(y+\omega,y)[e^{-\beta y} - e^{-\beta(y+\omega)}] dy. \quad (6)$$

The partition function $Z = \int_{-\infty}^{\infty} \rho(E)\exp(-\beta E)$ is easily obtained by integrating over the density of states $\rho(E) = \sum_{n=0}^{D-1} \delta(E - E_n)$, which can be expanded in parallel to $\tilde{j}(x,y)$. Note the main advantage of this approach: The current operator density that enters the conductivity is the same for all temperatures, i.e., it needs to be expanded only once. Figure 1 exemplifies the different form of $\tilde{j}(x,y)$ in the weak and strong EP coupling regimes.

At very low temperatures, the numerical evaluation of expression (6) requires some caution, since the Boltzmann factors heavily amplify small numerical errors in $j(y+\omega,y)$. We can avoid these problems, occurring mainly at the lower bound of the spectrum, by treating the contributions of the ground state and some of the lowest excitations separately. This is illustrated in Fig. 2. We split the optical conductivity into three parts,

$$\text{Re }\sigma(\omega) = \text{Re }\sigma^{\text{ED}}(\omega) + \text{Re }\sigma_{\text{KPM}}^{\text{1D}}(\omega) + \text{Re }\sigma_{\text{KPM}}^{\text{2D}}(\omega), \quad (7)$$

where the first contribution describes the transitions (matrix elements) between the S separated eigenstates, the second part those between the separated states and the rest of the spectrum, which can be expressed as standard 1D KPM expansions, and finally the transitions within the remaining $D-S$ states of the spectrum, handled by a 2D expansion.
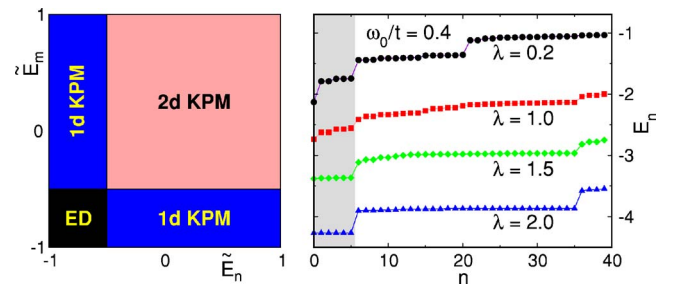

FIG. 2. (Color online) Schematic setup for the calculation of the finite-temperature optical conductivity (left panel). Lowest eigenvalues of the Holstein Hamiltonian for $L=6$, $M=25$, and PBC (right panel). The shaded area marks the six lowest eigenvalues to be separated from the rest of the spectrum.
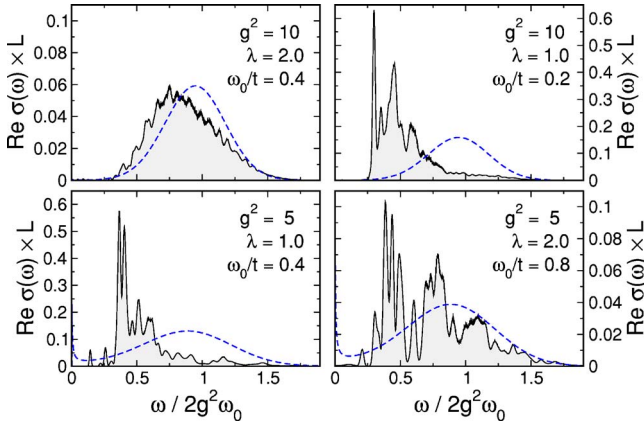
FIG. 3. (Color online) Optical conductivity in the 1D Holstein model at $T=0$ (in units of $\pi e^2 t^2$) compared to the analytical small polaron result Eq. (8) (dashed blue lines). Exact diagonalization data (ED) are obtained for a system with $L=6$ and $M=45$; σ_0 is determined to give the same integrated spectral weight of the $\omega>0$ (regular part) of Re σ.

Using the projection operator $P=1-\Sigma_{s=0}^{S-1}|s\rangle\langle s|$, the moments for the contributions Re $\sigma_{1D}(\omega)$ read $\mu_k^n=\langle n|\hat{j}PT_k(\tilde{H})P\hat{j}|n\rangle$. Of course, the number of states one has to separate depends on the physical situation. The right panel of Fig. 2 gives the lowest eigenvalues of the Holstein model at various coupling strengths. In the strong coupling regime ($\lambda\gg1$) states belonging to the lowest small polaron band have almost the same energy as the ground state and therefore should be treated separately (cf. the curves for $\lambda=1.5$ and 2). Obviously the situation is far less dramatic at weak EP couplings.

III. NUMERICAL RESULTS AND DISCUSSION

A. ac conductivity

We now apply our numerical scheme to the calculation of the optical absorption in the 1D Holstein model. The results for Re $\sigma(\omega)$ and possible deviations from established polaron theory are important for relating theory and experiment. The standard description of small polaron transport[4,25] provides the ac conductivity at $T=0$ as

$$\text{Re } \sigma(\omega) = \frac{\sigma_0}{\sqrt{\varepsilon_p\omega_0}}\frac{1}{\omega}\exp\left[-\frac{(\omega-2\varepsilon_p)^2}{4\varepsilon_p\omega_0}\right]. \quad (8)$$

For sufficiently strong coupling, this formula predicts a weakly asymmetric Gaussian absorption peak centered at $\omega=2\varepsilon_p$. A similar analytical formula can be derived for finite temperatures.[18,26]

Starting at *zero temperature*, Fig. 3 shows Re $\sigma(\omega)$ for various EP parameters. For $\lambda=2$ and $\omega_0/t=0.4$, i.e., at rather large EP coupling, but not in the extreme small polaron limit, we find also a pronounced maximum in the low-temperature optical response, which, however, is located somewhat below $2\varepsilon_p=2g^2\omega_0$, being the value for small polarons at $T=0$. At the same time, the line shape is more asymmetric than in standard polaron theory, with a weaker decay at the high-energy side, which fits even better the experimental behavior
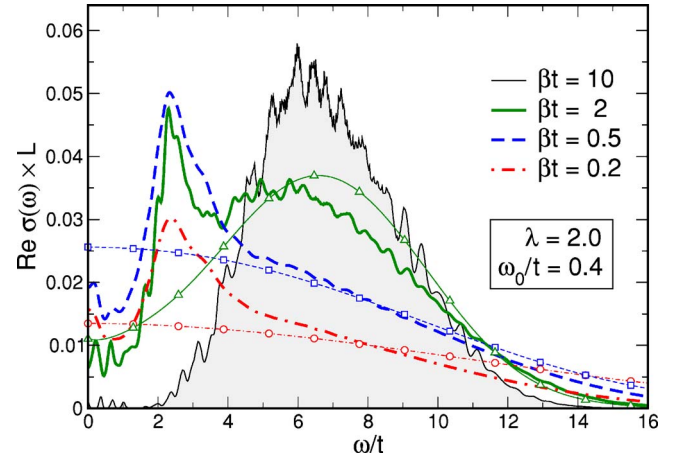

FIG. 4. (Color online) Optical absorption by Holstein polarons at finite temperatures in the adiabatic regime ($L=6$, $M=45$). Thin lines with symbols give the analytical results for the small polaron transport (Refs. 18 and 26) at temperatures $\beta t=2$ (triangles), 0.5 (squares), 0.2 (circles). The deviations observed for high excitation energies at very large temperatures are caused by the necessary truncation of the phonon Hilbert space in ED.

observed in polaronic materials such as TiO_2.[27] Varying the parameters, significant discrepancies to a Gaussian-like absorption are found. Then the polaron motion is not adequately described as hopping of a self-trapped carrier almost localized on a single lattice site.

At *finite temperature* two different transport mechanisms can be distinguished. Clearly, coherent transport, which for large EP couplings is related to diagonal (zero-phonon) transitions within the lowest extremely narrow polaron band, will be negligible at high temperatures. For instance, the amplitude of the current matrix elements between the degenerate states with momentum $K=\pm\pi/3$ ($K=0$, $\pm\pi/3$, $\pm2\pi/3$, and π are the allowed wave numbers of a six-site system with PBC) is of the order of 10^{-7} only. Whereas phase coherence is maintained during a diagonal transition, the particle loses its phase coherence if its motion is triggered by (multi-)phonon absorption and emission processes. These so-called nondiagonal transitions which, of course, can take place also with zero-energy transfer, become more and more important as the temperature increases. Accordingly the main transport mechanism is thermally activated hopping, where each hop becomes a statistically independent event. In the small polaron limit, where the polaronic subbands are roughly separated by the bare phonon frequency (cf. Fig. 2, right panel), this happens for $T\gtrsim\omega_0$. Let us consider the activated regime in more detail (cf. Fig. 4): With increasing temperatures we observe a substantial spectral weight transfer to lower frequencies, and an increase of the zero-energy transition probability in accordance with previous results.[28]

In addition, we find a strong resonance in the absorption spectra at about $\omega\sim2t$, which can be easily understood using a configurational coordinate picture. Placing a homogeneous lattice distortion u at L_u consecutive sites by applying the unitary transformation $S^\dagger(u)=\Pi_i^{L_u}S_i^\dagger(u)=\Pi_i^{L_u}\exp[u(b_i^\dagger-b_i)]$, the transformed Holstein Hamiltonian takes the form $\bar{H}=\langle0|S^\dagger(u)HS(u)|0\rangle_{ph}=-t\Sigma_{\langle i,j\rangle}c_i^\dagger c_j-2\sqrt{\varepsilon_p\omega_0}u\Sigma_i^{L_u}n_i+\omega_0u^2L_u$.
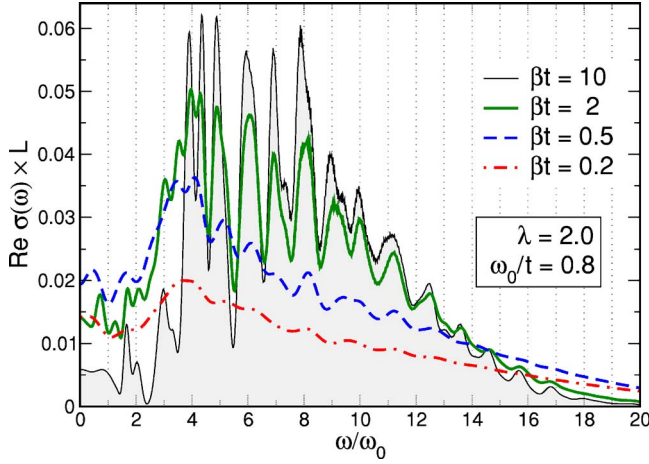
FIG. 5. (Color online) Optical absorption by Holstein polarons at finite temperatures in the nonadiabatic regime ($L=6$, $M=30$). Note that now the abscissa is scaled with respect to the phonon frequency.

In the adiabatic strong-EP coupling regime, the ground state can be approximated as an electron localized at a certain single site with the lattice being in a shifted oscillator state ($L_u=1$). That is, $|\Psi_0\rangle=|1\rangle_{el}\otimes S_1^\dagger(g)|0\rangle_{ph}$ and $E_0=-\varepsilon_p$, in accordance with the Lang-Firsov approximation. Now let us consider excitations from this ground state, where the lattice distortion spreads over two neighboring sites ($L_u=2$) and the electron is in a symmetric or antisymmetric linear combination of $|1\rangle_{el}$ and $|2\rangle_{el}$, i.e., the particle is mainly located at sites 1 and 2 but delocalized between these sites. We then find $|\Psi_{1,\pm}\rangle=(|1\rangle_{el}\pm|2\rangle_{el})\otimes S_2^\dagger(g/2)S_1^\dagger(g/2)|0\rangle_{ph}$ and $E_{1,\pm}=\mp t-\varepsilon_p/2$. Whereas the (potential) energy related to the displacement field is reduced to $-\varepsilon_p/L_u$, the kinetic energy comes into play since hopping processes between 1 and 2 are allowed. The current operator $\hat{j}$ connects these different-parity states with perfect overlap $|\langle\Psi_{1,+}|\hat{j}|\Psi_{1,-}\rangle|^2=(et)^2$, giving rise to a strong signal in the optical absorption. Note that the excitation energy $\omega_{1-,1+}=2t$ is independent of ε_p. In order to activate these transitions thermally, the electron has to overcome the "adiabatic" barrier $\Delta=E_{1+}-E_0=\varepsilon_p/2-t$. A finite phonon frequency will relax this condition. From Fig. 4, we find the signature to occur above $T\gtrsim 0.5t$. Obviously this feature is absent in the standard small-polaron transport description which essentially treats the polaron as a quasiparticle without resolving its internal structure. Owing to the infinite number of neighboring sites it is also absent in the DMFT calculation. Of course, one could also extend this scenario to excitations where the electron is delocalized over more than two distorted lattice sites, but for the present parameters the signature of these weakly bound states would be rather small.

Entering the nonadiabatic regime of large phonon frequencies at fixed $\lambda=2$, the pattern of subbands separated roughly by ω_0 becomes more pronounced, but is, of course, washed out at higher temperatures (see Fig. 5 for $\omega_0/t=0.8$). In Fig. 5 the average number of phonons contained in the ground state ($\propto g^2$) is smaller ($g^2=5$) than in the previous case where $g^2=10$ ($\omega_0/t=0.4$). This also concerns the acti-
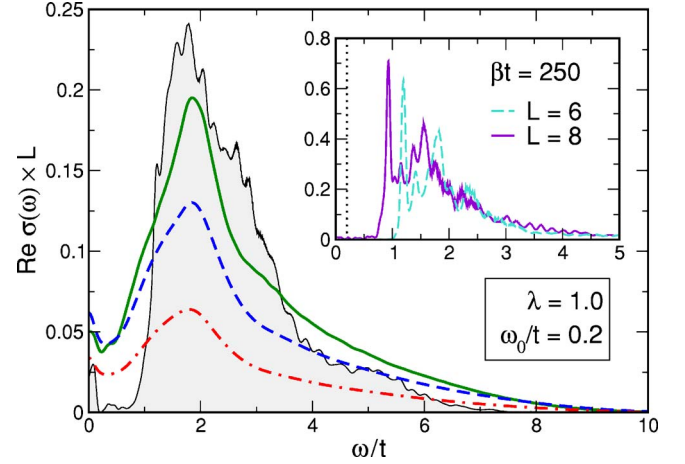

FIG. 6. (Color online) Optical absorption in the adiabatic intermediate EP coupling regime (the notation is the same as in Fig. 4; again we use $L=6$, $M=40$). The inset illustrates the finite-size dependence of Re $\sigma(\omega)$ for $T\sim 0$ (the vertical dotted line gives the phonon absorption threshold). It demonstrates that the gap observed at low frequencies and temperatures is clearly a finite-size effect, i.e., at weak to intermediate couplings, the discrete electronic levels of our finite system show up in the conductivity spectra. These effects, of course, are of minor importance at larger EP couplings, where the polaronic bandwidth is strongly reduced, as well as for high temperatures.

vated region $\omega_0/t\lesssim T\lesssim\Delta$ but for these parameters the simple adiabatic picture anticipated above breaks down anyway.

Now let us decrease the EP coupling strength at small phonon frequencies $\omega_0/t=0.2$ keeping $g^2=10$ fixed. Results for the optical response in the vicinity of the large to small polaron crossover ($\lambda=1$) are depicted in Fig. 6. Here the small-polaron maximum has almost disappeared and the $2t$-absorption feature can be activated at very low temperatures ($\Delta\to 0$ for the two-site model with $\lambda=1$). The overall behavior of Re $\sigma(\omega)$ resembles that of polarons of intermediate size. At high temperatures these polarons will dissociate readily and the transport properties are equivalent to those of electrons scattered by thermal phonons. Let us emphasize that many-polaron effects become increasingly important in the large-to-small polaron transition region.[29] As a result, polaron transport might be changed entirely compared to the one-particle picture discussed so far.

B. Sum rules

Before we consider the temperature dependence of the dc conductivity, it is useful to test the sum rules for the real part of the optical response. First we have the so-called *f*-sum rule,

$$S_{\text{tot}}:=\int_{-\infty}^\infty \text{Re } \sigma(\omega)d\omega=-\frac{\pi e^2}{L}E_{\text{kin}}, \qquad (9)$$

which relates the ω-integrated Re $\sigma(\omega)$ to the kinetic energy $E_{\text{kin}}=-t\sum_{\langle i,j\rangle}\langle c_i^\dagger c_j\rangle_T$. Note that the $\omega=0$ (Drude) contribution is included in (9). The second sum rule for Re $\sigma(\omega)$ is
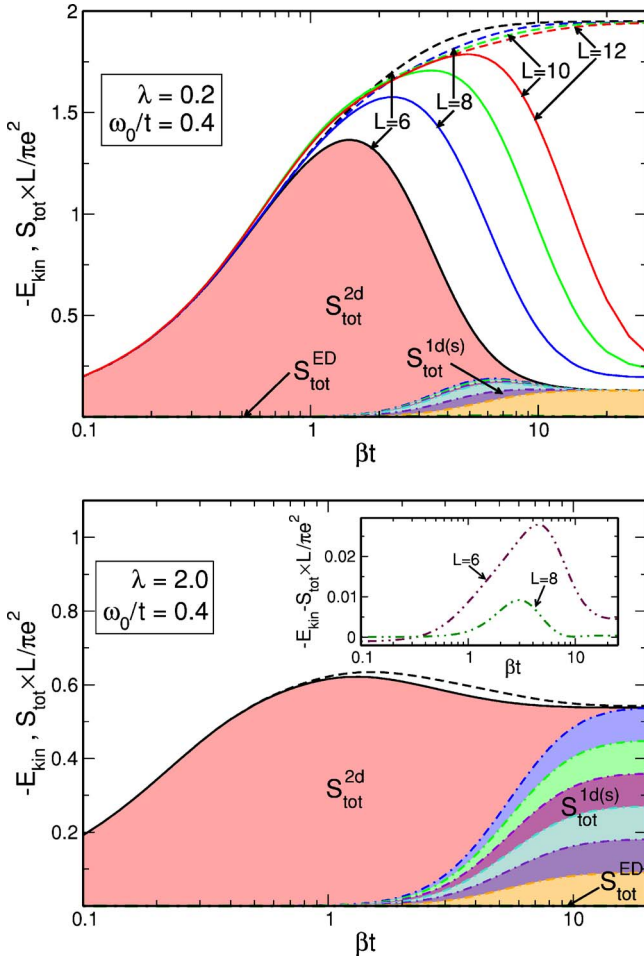
FIG. 7. (Color online) Conformance of the f-sum rule (9) in the weak (upper panel) and strong (lower panel) EP coupling regimes of the 1D Holstein model. Results for S_{tot}, partial S_{tot}'s and E_{kin} are given by solid, dot-dashed, and dashed lines, respectively. For further explanation see text.

$$\int_0^\infty \omega\, \mathrm{Re}\,\sigma(\omega)\,d\omega = \frac{\pi}{L}\langle \hat{j}^2 \rangle_T. \qquad (10)$$

Throughout our calculations Eq. (10) was fulfilled within numerical accuracy, where the thermal average $\langle \hat{j}^2 \rangle_T$ was determined again using a 1D KPM. Testing sum rule (9) we gain important information about finite-size effects.

Figure 7 compares E_{kin} and $S_{tot}L/\pi e^2$ obtained from our finite-cluster calculation. At weak EP couplings the kinetic energy is a strictly monotonic increasing function of temperature and becomes strongly suppressed at high temperatures due to scattering of the electron by thermal phonons. Whereas the f-sum rule is almost perfectly fulfilled for smaller values of β, we found pronounced deviations at low temperatures which, without doubt, can be assigned to the finite size of our Holstein ring (cf. the L dependence of S_{tot} shown in the upper panel of Fig. 7, and also the discussion of the dc conductivity below). Clearly finite-size effects become important when the temperature is comparable to the energy gaps in the spectrum of H (see Fig. 2). At strong EP cou-

plings the transport is hopping-dominated and the kinetic energy exhibits a maximum at a finite temperature that can be related to the thermal activation energy of polarons. Now, in view of the narrow small polaron band (cf. Fig. 2), finite size gaps are small and the f-sum rule is fulfilled down to very low temperatures. Small deviations appear to vanish rapidly with increasing system size (see inset, lower panel of Fig. 7). In order to analyze the contributions of different transport processes to E_{kin} in some more detail, we have decomposed $S_{tot}=S_{tot}^{ED}+\Sigma_{s=0}^{S-1}S_{tot}^{1D(s)}+S_{tot}^{2D}$ in analogy to Eq. (7). Figure 7 shows that the coherent (intraband) contribution ($\propto S_{tot}^{ED}$) is almost negligible at the temperatures considered. Interband transitions connecting eigenstates of the lowest polaron band to higher excited states (1D KPM) are the determining factor at low T. If the renormalized polaron bandwidth is small enough, all states in the band are equally populated, leading to pretty much the same values of $S_{tot}^{1D(s)}$. At high temperatures, of course, the transitions covered by the 2D KPM are predominant.

C. dc conductivity

The dc conductivity is obtained by taking the limit $\omega \to 0$ of (3), which with $\lim_{\omega \to 0}(1-e^{-\beta\omega})/\omega=\beta$ yields

$$\mathrm{Re}\,\sigma_{dc} = \frac{\pi\beta}{ZL}\sum_{n,m}^{D-1} e^{-\beta E_n}|\langle n|\hat{j}|m\rangle|^2 \delta(E_m - E_n). \qquad (11)$$

$\mathrm{Re}\,\sigma_{dc}$ essentially counts the number of thermally accessible current carrying (degenerate) states. Since we have $\langle 0|\hat{j}|0\rangle = 0$ the conductivity almost vanishes for small T below the finite-size gap between the ground state and the first excited state. In the thermodynamic limit, $L \to \infty$, $\mathrm{Re}\,\sigma_{dc}$ is related to the charge stiffness D_c, or the so-called Drude weight (at $T=0$).[30]

The temperature dependence of the dc conductivity is illustrated in Fig. 8. Again the weak coupling results appear to have a rather strong finite-size dependence (note that $\mathrm{Re}\,\sigma_{dc}$ depicted in Fig. 8 is an intensive quantity). When L increases, a pronounced signature develops at low temperatures. Independent of the coupling strength ε_p, the polaron is still an itinerant quasiparticle that, for $T \to 0$, gives rise to band conduction. Thus, for $L \to \infty$, we expect metallic behavior as indicated by the DMFT results depicted in the lower panel.

The shoulder observed for the 10 and 12 site systems at $T/t \gtrsim 1$, again is an artifact of our phonon truncation procedure as can be seen by comparing the data obtained for $L=6$ and different numbers of the phonon cutoff M. In the strong EP-coupling polaronic regime, bandlike transport becomes extensively suppressed (the Drude weight is exponentially small). Nevertheless quantum zero-point phonon fluctuations cause polaron delocalization at $T=0$. At higher temperatures incoherent polaron hopping transport manifests in the temperature dependence, leading to the well-known absorption maximum in $\mathrm{Re}\,\sigma_{dc}(T)$ (cf. Fig. 8, lower panel). Since this signature is related to (rather local) polaron excitation processes, the position of the maximum is almost independent of the system size. In comparison to the $D=\infty$
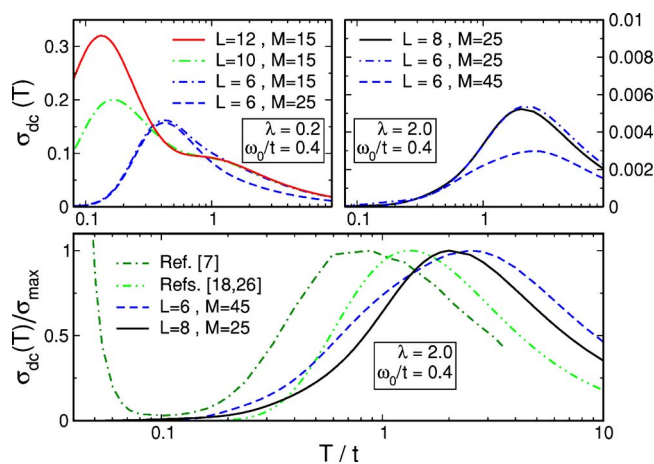
FIG. 8. (Color online) Top row: DC conductivity as a function of temperature at weak (left panel) and strong (right panel) EP coupling. The bottom panel shows, for strong coupling, a comparison with recent DMFT results (Ref. 7) and standard polaron theory (Refs. 18 and 26) (for $T \gtrsim \omega_0/2$). ED data do not account for the low-energy tail because of the finiteness of the system.

(DMFT) results[7] we find the same qualitative behavior in the relevant temperature regime $\omega_0 \lesssim T \sim 2\varepsilon_p$ but a different location of the conductivity maximum. Generally in DMFT the activation energy for polaron hopping turns out to be lower than expected from commonly accepted arguments for finite-dimensional systems. Increasing the lattice size, our 1D Holstein data indicate that this discrepancy does not necessarily imply the failure of standard theory of hopping conduction[26] but may partly arise from dimensionality effects on polaron transport in infinite dimensions. Conversely, and in light of the deviations found for the ac conductivity (cf. Fig. 4), the standard (antiadiabatic) strong coupling description can only be supposed to provide estimates on relevant energy scales in the intermediate adiabatic EP-coupling regime.

IV. SUMMARY

In this work, we have investigated the motion of a charge carrier in response to ac and dc external fields for strongly correlated 1D electron-phonon systems. The combination of Lanczos diagonalization and the kernel polynomial method has enabled us to calculate for the first time quasi-exactly the temperature dependence of the optical absorption spectra and the dc conductivity in the framework of the one-dimensional Holstein model. Besides the well-known polaron maximum, a pronounced absorption feature at about $2t$ is found in the optical conductivity. Finite-size effects were identified and assessed, e.g., on the basis of the f-sum rule. In the physically most interesting range of intermediate coupling strengths and phonon frequencies, we find that the conductivity deviates from the standard small polaron results.

[1] A. R. Bishop and B. I. Swanson, Los Alamos Sci. **21**, 133 (1993); H. Fehske, M. Kinateder, G. Wellein, and A. R. Bishop, Phys. Rev. B **63**, 245121 (2001).

[2] E. Dagotto, Rev. Mod. Phys. **66**, 763 (1994); S. Tajima, Y. Fudamoto, T. Kakeshita, B. Gorshunov, V. Železny, K. M. Kojima, M. Dressel, and S. Uchida, Phys. Rev. B **71**, 094508 (2005).

[3] S. Jin, T. H. Tiefel, M. McCormack, R. A. Fastnach, R. Ramesh, and L. H. Chen, Science **264**, 413 (1994); A. Weiße and H. Fehske, New J. Phys. **6**, 158 (2004).

[4] D. Emin, Phys. Rev. B **48**, 13691 (1993).

[5] A. S. Alexandrov and N. F. Mott, *Polarons and Bipolarons* (World Scientific, Singapore, 1995).

[6] D. C. Worledge, L. Miéville, and T. H. Geballe, Phys. Rev. B **57**, 15267 (1998).

[7] S. Fratini, F. de Pasquale, and S. Ciuchi, Phys. Rev. B **63**, 153101 (2001); S. Fratini and S. Ciuchi, Phys. Rev. Lett. **91**, 256403 (2003).

[8] H. Fehske, J. Loos, and G. Wellein, Z. Phys. B: Condens. Matter **104**, 619 (1997); G. Wellein and H. Fehske, Phys. Rev. B **58**, 6208 (1998); H. Fehske, J. Loos, and G. Wellein, *ibid.* **61**, 8016 (2000).

[9] C. Zhang, E. Jeckelmann, and S. R. White, Phys. Rev. B **60**, 14092 (1999).

[10] R. N. Silver, H. Röder, A. F. Voter, and D. J. Kress, J. Comput. Phys. **124**, 115 (1996).

[11] A. Weiße, G. Wellein, A. Alvermann, and H. Fehske, cond-mat/0504627 (unpublished).

[12] T. Holstein, Ann. Phys. (N.Y.) **8**, 325 (1959); *ibid.* **8**, 343 (1959).

[13] G. Wellein and H. Fehske, Phys. Rev. B **56**, 4513 (1997).

[14] M. Capone, W. Stephan, and M. Grilli, Phys. Rev. B **56**, 4484 (1997).

[15] D. Emin, Phys. Rev. B **33**, 3973 (1986); V. V. Kabanov and O. Y. Mashtakov, *ibid.* **47**, 6060 (1993).

[16] H. Fehske, H. Röder, G. Wellein, and A. Mistriotis, Phys. Rev. B **51**, 16582 (1995); L.-C. Ku, S. A. Trugman, and J. Bonča, *ibid.* **65**, 174306 (2002).

[17] V. Cataudella, G. De Filippis, and G. Iadonisi, Phys. Rev. B **60**, 15163 (1999); *ibid.* **63**, 052406 (2001).

[18] G. D. Mahan, *Many-Particle Physics* (Kluwer Academic/Plenum Publishers, New York, 2000).

[19] B. Bäuml, G. Wellein, and H. Fehske, Phys. Rev. B **58**, 3663 (1998).

[20] O. S. Barišić, Phys. Rev. B **65**, 144301 (2002); H. Fehske, M. Sekania, A. P. Kampf, and G. Wellein, Eur. Phys. J. B **31**, 11 (2003).

[21] I. G. Lang and Y. A. Firsov, Zh. Eksp. Teor. Fiz. **43**, 1843 (1962);

Y. A. Firsov, *Polarons* (Izd. Nauka, Moscow, 1975); Y. A. Firsov, Semiconductors **29**, 515 (1995).

[22] A. Weiße, Eur. Phys. J. B **40**, 125 (2004).

[23] D. Jackson, Trans. Am. Math. Soc. **13**, 491 (1912).

[24] D. A. Drabold and O. F. Sankey, Phys. Rev. Lett. **70**, 3631 (1993).

[25] H. G. Reik and D. Heese, J. Phys. Chem. Solids **28**, 581 (1967).

[26] H. Böttger and V. V. Bryksin, *Hopping Conduction in Solids* (Akademie Verlag, Berlin, 1985).

[27] E. K. Kudinov, D. N. Mirlin, and Y. A. Firsov, Fiz. Tverd. Tela (Leningrad) **11**, 2789 (1969) [Sov. Phys. Solid State **11**, 2257 (1970)].

[28] E. L. Nagaev, Sov. Phys. Solid State **4**, 1611 (1963).

[29] M. Hohenadler, D. Neuber, W. von der Linden, G. Wellein, J. Loos, and H. Fehske, Phys. Rev. B **71**, 245111 (2005).

[30] B. S. Shastry and B. Sutherland, Phys. Rev. Lett. **65**, 243 (1990); B. N. Narozhny, A. J. Millis, and N. Andrei, Phys. Rev. B **58**, R2921 (1998).